Magnetic structure of $NdMnO_3$ consistently doped with Sr and Ru

A. M. Balagurov and S. N. Bushmeleva*
Frank Laboratory of Neutron Physics, JINR, 141980 Dubna, Russia

V. Yu. Pomjakushin† and D. V. Sheptyakov
Laboratory for Neutron Scattering, ETH Zürich & Paul Scherrer Institute, 5232 Villigen PSI, Switzerland

V. A. Amelichev, O. Yu. Gorbenko, A. R. Kaul, and E. A. Gan'shina
Department of Chemistry, Moscow State University, Moscow 119899, Russia

N. B. Perkins
Bogolyubov Laboratory of Theoretical Physics, JINR, 141980 Dubna, Russia
(Received 30 April 2003; revised manuscript received 10 March 2004; published 23 July 2004)

The crystal and magnetic structures of the $(Nd_{1-x}Sr_x)(Mn_{1-x}Ru_x)O_3$ perovskites have been studied by neutron powder diffraction and muon spin relaxation. The simultaneous and consistent doping of the A- and B-sites with Sr and Ru has been used for avoiding the Mn^{4+} formation and hence, suppression of the double exchange. All studied samples ($0 \leqslant x \leqslant 0.875$) are insulators and show unusual long-range ferromagnetic state, which can be called "statistical ferrimagnet," with antiferromagnetic coupling between Mn and Ru magnetic moments, and ferromagnetic coupling in the Mn-Mn and Ru-Ru pairs.

DOI: 10.1103/PhysRevB.70.014427 PACS number(s): 75.30.−m, 61.12.Ld

I. INTRODUCTION

Rare earth perovskite manganites of $LaMnO_3$ type continue to be a subject of intensive studies. Upon A-site (substitution of La for Ca or other divalent alkaline earth cations) or B-site (substitution of Mn for Co or other 3*d* or 4*d* cations) doping, the manganites exhibit a wide variety of physical properties including colossal magnetoresistance effect (CMR) observed in the family near the temperature of the ferromagnetic ordering, T_C (see, for instance, recent reviews[1,2]). Historically, more attention was paid to A-site substitution, leading to appearance of intermediate or mixed Mn^{3+}/Mn^{4+} valence states of Mn ions. It has been observed that the metallic phase appeared with doping at low temperatures concomitantly with ferromagnetic ordering. These studies have established that the basic model for understanding of coexistence of the ferromagnetism (FM) and metalicity is the double-exchange model introduced a long time ago by Zener,[3] in which strong FM exchange interaction between the localized magnetic moments of Mn^{3+} and Mn^{4+} cations is mediated by the hopping of e_g-electrons. However, there are some experimental evidences that the ferromagnetism itself is not necessarily connected with DE interactions.[4]

The substitution of Mn, or B-site doping, has been much more rarely examined so far. However, it may provide new insights into the understanding of physics in these CMR compounds. In particular, substitution of Mn for Ru is especially interesting because it leads to some unusual consequences both in transport and magnetic properties.[5–8] The 4*d*-ion of ruthenium has more extended and, therefore, less localized 4*d*-orbitals than the Mn 3*d*-orbitals, and thus the partial overlapping of the Ru 4*d*-orbitals with the oxygen 2*p*-orbitals is similar and even stronger as compared to the 3*d*-orbitals of Mn. Indeed, $SrRuO_3$ and $CaRuO_3$ are metals and the first one is also ferromagnetic with a high magnetoresistance in the vicinity of Curie temperature.[9] Another important feature of Ru ion is that its (4*d*) configuration has a reference energy close enough to one of (3*d*) Mn ion and the hybridization between the orbitals can be strong. Therefore, superexchange interaction between Mn and Ru is large and can significantly affect the physical properties of Ru-doped manganites.

Exceptional ability of ruthenium to induce metallicity and ferromagnetism has been discovered for wide composition and doping range of manganites, from the hole rich to the electron rich side. Raveau *et al.*[6,10] have shown that substitution of Mn for Ru (at least up to 12% level) in $R_{1-y}Ca_yMnO_3$ (R is rare earth element), favors the appearance of FM state and improves their metallic properties. One of the most spectacular effects has been observed for $Sm_{0.4}Ca_{0.6}Mn_{1-y}Ru_yO_3$ series,[5] where the antiferromagnetic charge ordered phase was readily destroyed by the Ru-doping being replaced by the ferromagnetic metallic state. One of possible explanations of the extreme efficiency of the Ru-doping in inducing the ferromagnetic metallic state in the charge ordered manganites is the possibility for ruthenium to exhibit a mixed valence.[5] The substitution of manganese ions Mn^{3+} can be made either by Ru^{3+}, Ru^{4+}, or Ru^{5+} species.[6,11,12] However, the experimental data on the Ru electronic states in manganites contradict each other. Raveau *et al.*[10] believe that in mixed manganites, only Ru^{4+} and Ru^{5+} are possible, while XPS (x-ray photoelectron spectroscopy)[11] and x-ray diffraction studies[12] suggest Ru^{3+}/Ru^{4+} mixed state. In any case, mixed-valence ruthenium ion can cause orbital reorientation and spin reversal of Mn cations in the antiferromagnetic structures together with strong charge fluctuations (Mn^{3+}/Mn^{4+}) around Ru ion, which should induce the formation of the ferromagnetic metallic clusters.[5] This behavior could be still understood by extension of the double exchange model involving both mixed-valence Mn and Ru

ions even if the exact role of Ru doping on the properties of manganites remains still an open problem.

The experimental approach we propose here is an investigation of manganite compounds for which DE-mechanism is weakened or even completely eliminated. It might be realized by the simultaneous and consistent doping in both A- and B-sublattices of the perovskite structure with di- and four-valence ions, respectively. This kind of doping may allow the realization of the fixed value of the Mn oxidation state (Mn^{3+}) and consequently, switching off the double exchange interaction between Mn-ions. We have studied effect of this doping in $(Nd_{1-x}Sr_x)(Mn_{1-x}Ru_x)O_3$, considering ruthenium being predominantly four-valence Ru^{4+} in the low-spin $t_{2g}(4d)$ configuration which is favorable due to prevailing of the crystal field splitting over the intra-atomic Hund interactions in the 4*d*-band. The results obtained differ significantly from the results of the previous studies of manganites doped with Ru. We conclude that introducing the equal amounts of Sr and Ru results in an asymmetric phase diagram with stabilization of the unusual insulating ferromagnetic state with antiparallel ordering of magnetic moments in Mn-Ru pairs and with total suppression of the transition to the metallic state.

II. SAMPLE EXPERIMENTAL

The single phase $(Nd_{1-x}Sr_x)(Mn_{1-x}Ru_x)O_{3+\delta}$ powder samples ($x=0$, 0.125, 0.25, 0.5, 0.75, 0.875, 1.0, $\delta \approx 0$) have been prepared in the ceramic state with the use of the chemical homogenization method. First, ash-free paper was soaked with the water solution of Nd, Sr and Mn nitrates, mixed in the proper ratio, and dried in air at 120 °C. Then paper was burned, and the ash was annealed in the air at 700 °C during 30 minutes. Resulting powder was mixed with RuO_2 powder and pressed in pellets. Sintering was accomplished at 1200 °C in air for 16 hours.

Electron probe microanalysis shows satisfactory agreement of the calculated and experimentally measured cation stoichiometry. All the samples with $x \leqslant 0.875$ reveal semiconducting behavior of the electric resistivity without any peculiarities at the magnetic ordering temperature (Fig. 1). However, in the whole temperature range, the electrical resistance and the conduction activation energy decrease significantly with increasing x. This corresponds to approaching the $x=1$ composition which is metallic. Iodometric titration was accomplished as described in Ref. 13. The oxygen nonstoichiometry index for $x=0$ composition was found to be 0.01 but the other compositions reveal higher deviation of the oxygen index from 3.0 ($\delta \approx 0.10$ for $x=0.25$ and $\delta \leqslant 0.06$ for other samples). Thus, the agreed character of doping in A- and B-sublattices of the perovskite structure is somewhat distorted. According to Ref. 6 in manganites containing ruthenium, the doped holes are mostly captured by ruthenium instead of manganese. It means that for oxygen index $3+\delta$, 2δ ions of Ru^{4+} are transformed to Ru^{5+}, and the extracted magnetic moment of Ru should be regarded as amount of $(x-2\delta)\mu(Ru^{4+})$ and $2\delta\mu(Ru^{5+})$. At the same time, it is known that the insertion of excess oxygen is not possible in three-dimensional (3D) perovskite structure and the oxygen nonstoichiometry in a sample is incorporated via cation vacancies, with equal amounts in A- and B-sites (see, for instance, Ref. 14). The number of vacancies γ in each site can be calculated according to $\gamma=\delta/(3+\delta)$, i.e., even for $\delta=0.1$, γ is around 0.03, which is at the level of experimental uncertainties in occupation factors. For this reason we used fully occupied A- and B-sites in the Rietveld refinements for all samples.

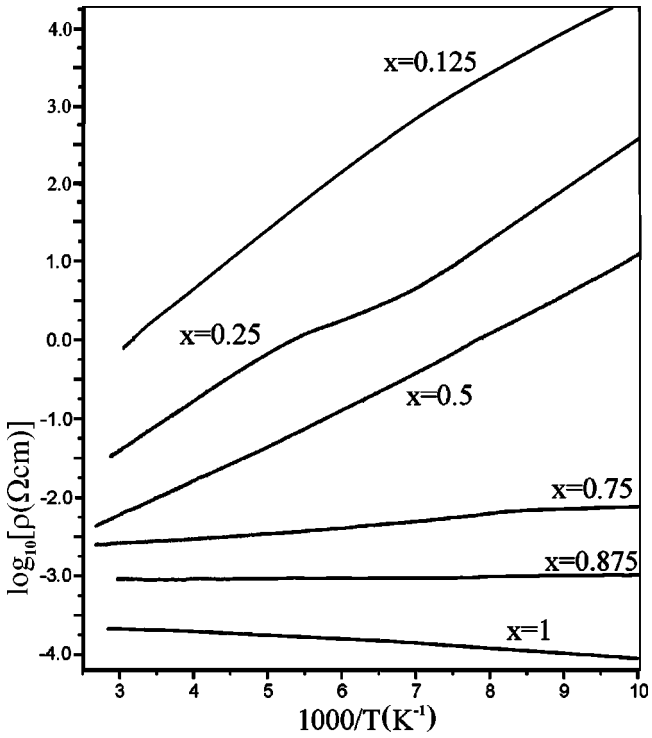

FIG. 1. Temperature dependence of the electrical resistivity of the ceramic samples of $(Nd_{1-x}Sr_x)(Mn_{1-x}Ru_x)O_3$. All the samples with $x \leqslant 0.875$ reveal semiconduction behavior.

The magnetic susceptibility was measured in the field of 10–20 Oe at several frequencies between 100 and 1000 Hz. For all samples the frequency dependence of the susceptibility is negligibly small. The compositions with x between 0.125 and 0.5 demonstrate the ferromagnetic type behavior of the magnetic susceptibility (Fig. 2) with one pronounced phase transition. For $x=0.75$ and 0.875 together with the ferromagnetic transition one can see an additional transition at lower temperatures. It will be discussed later together with μSR data.

Neutron diffraction (ND) experiments have been performed at several instruments: HRFD at FLNP, JINR at the IBR-2 pulsed reactor, HRPT[15] and DMC at the SINQ spallation source of Paul Scherrer Institut (Villigen, Switzerland). At high resolution diffractometers HRFD and HRPT crystal structure of the samples with $0 \leqslant x \leqslant 0.875$ have been studied. Medium resolution DMC instrument was used for magnetic structure studies of all samples except $x=0$ and 1. The diffraction patterns were measured in the regime of heating in the wide temperature range. For the Rietveld refinements, MRIA[16] and FULLPROF[17] programs were used. The data on crystal structure were treated in the conventional for manganites with $\langle r_A \rangle \approx 1.2$ *Å* orthorhombic space group *Pnma* in

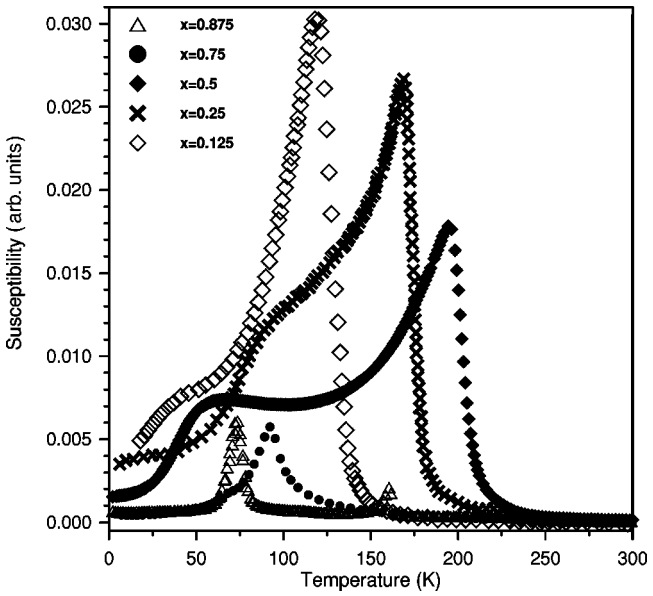

FIG. 2. Temperature dependence of the magnetic susceptibility of the $x=0.125$, 0.25, 0.50, 0.75, and 0.875 compositions.

the standard setting ($a \approx c \approx \sqrt{2}a_c \approx 5.4$ *Å*, $b \approx 2a_c \approx 7.6$ *Å*, where $a_c \approx 3.8$ *Å* is the lattice spacing of the ideal cubic perovskite). Typical high resolution neutron diffraction pattern and the Rietveld refinement for the sample with $x=0.5$ is shown in Fig. 3. More detailed description of $(Nd_{1-x}Sr_x) \times (Mn_{1-x}Ru_x)O_3$ compound preparation and characterization is given elsewhere.[18]

In further analysis we will limit ourselves to the properties of the $(Nd_{1-x}Sr_x)(Mn_{1-x}Ru_x)O_3$ with x greater than 0.1. The properties of $NdMnO_3$ in which there are both ferromagnetic and antiferromagnetic couplings between the Mn spins, resulting in a noncollinear structure below 75 K,[19] are quite different from the properties of the compositions with $x \geqslant 0.1$ being ferromagnets. The precision refinement of the $SrRuO_3$ crystal structure was done by Jones *et al.*[20] This

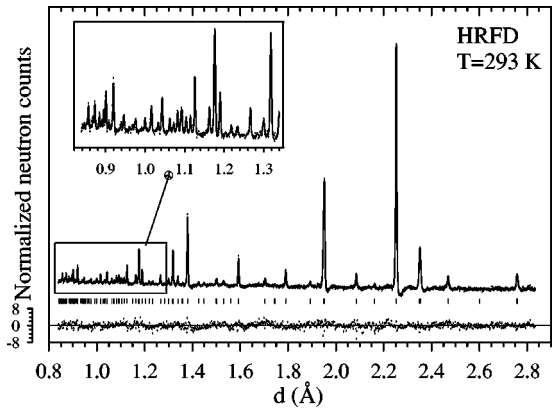

FIG. 3. Diffraction pattern of the $(Nd_{0.5}Sr_{0.5})(Mn_{0.5}Ru_{0.5})O_3$ sample, measured at the HRFD at room temperature and treated with Rietveld method. Experimental points, calculated profile and difference function are shown. The difference is normalized on the mean-square deviation for each point. Ticks below the graph indicate the calculated peak positions.

compound is known as a ferromagnet (see, for instance, Ref. 21) with $T_C=160$ K with saturation moment reported is between $\mu_{Ru}=1.1\ \mu_B$ obtained from the magnetization measurements in high magnetic field,[22] and $\mu_{Ru}=(1.4\pm0.4)\mu_B$ from neutron diffraction.[23]

III. RESULTS

A. Crystal structure

The partial substitution Nd and Mn for equal amounts of Sr and Ru leads at first to a sharp decrease of the unit cell volume and orthorhombic distortion ($a/c \approx 1.067$ and 1.011 for $x=0$ and 0.25 correspondingly), and equalizing of (Mn/Ru)-O interatomic distances. Upon further doping (x increases to 1), unit cell volume grows up practically linearly [Fig. 4(a)], oxygen octahedra become even more regular, i.e., all three independent bond lengths (Mn/Ru)-O1 (along b axes), (Mn/Ru)-O21 and (Mn/Ru)-O22 (in $a-c$ plane) converge at ~ 1.985 *Å*, which well corresponds to the Ru-O bonds in $SrRuO_3$. Both valence angles (Mn/Ru)-O1-(Mn/Ru) and (Mn/Ru)-O2-(Mn/Ru) are slowly increasing with x, which corresponds to the decrease of the oxygen octahedra tilt magnitudes both about b-axis and in the $a-c$ plane. This increase is consistent with the noticeable growth of the tolerance factor upon substitution of Nd^{3+} for Sr^{2+} and of Mn^{3+} for Ru^{4+}. These features, the most important of which is practical absence of the oxygen octahedra distortion starting from $x=0.25$, are illustrated in Fig. 4. Another important conclusion from the high-resolution neutron diffraction data is that there is no indication of either phase separation, or cation ordering. It means in particular that Mn substitution for Ru occurs statistically homogeneous. The Rietveld refinements of neutron diffraction data confirm also that Mn and Ru relative concentrations in B-sites are corresponding to the nominal stoichiometry. For instance, in the composition with $x=0.25$ the occupation factors for Mn and Ru are: $n(\mathrm{Mn})=0.760\pm0.008$, $n(\mathrm{Ru})=0.240\pm0.008$. Their ratio is equal to 3.17 ± 0.11, i.e., within $\approx 5\%$ limits is equal to 0.75:0.25. Since there is no proper way of distinguishing between Nd and Sr with neutrons, the ratio $n(\mathrm{Nd})/n(\mathrm{Sr})$ has been fixed to $n(\mathrm{Mn})/n(\mathrm{Ru})$.

For the $x=0.5$ sample the high-resolution diffraction patterns were measured in wide temperature range. Temperature dependencies of the structural parameters (lattice constants, interatomic distances, and valence angles) are quite monotonic (see, our paper, Ref. 18), which is conventional for manganites in an insulating state. The ferromagnetic phase transition at $T_C=200$ K is not revealed in these temperature dependencies.

B. Magnetic ordering

Comparison of the neutron diffraction patterns of $Nd_{0.5}Sr_{0.5}Mn_{0.5}Ru_{0.5}O_3$, measured at DMC at the room temperature and 10 K (Fig. 5) shows an increase in the intensity of some diffraction peaks due to the appearance of the FM contribution. No additional reflections were detected in the neutron diffraction patterns down to $T=8$ K. The similar behavior, appearance of FM order with the temperature de-

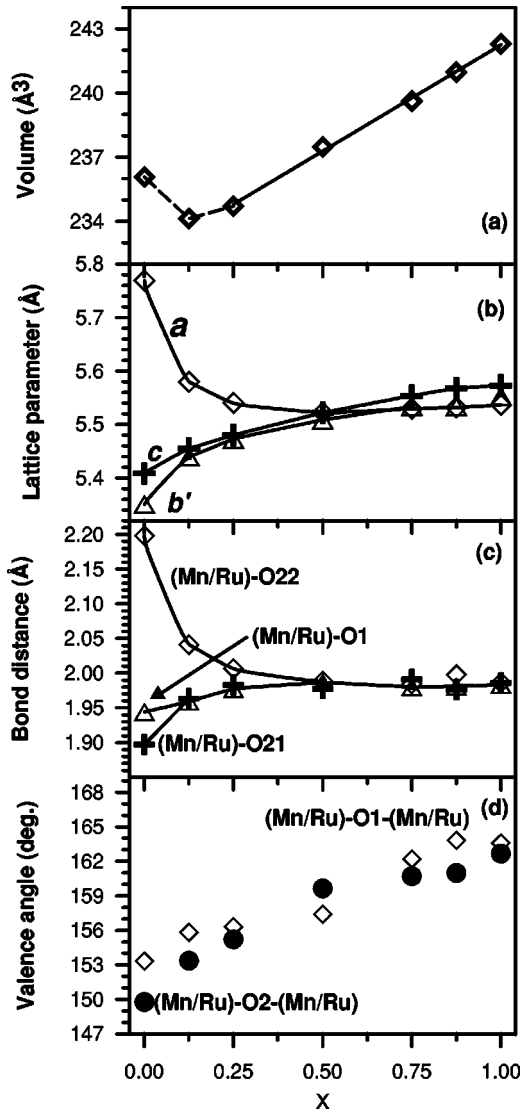

FIG. 4. Dependencies of the unit cell volume (a), the unit cell parameters ($b'=b/\sqrt{2}$) (b), the (Mn/Ru)-O bond lengths (c), and the (Mn/Ru)-O-(Mn/Ru) valence angles (d) of $(Nd_{1-x}Sr_x)(Mn_{1-x}Ru_x)O_3$ at room temperature on the (Sr,Ru) content x. Data for $x=1$ are taken from Ref. 20. The symbol sizes are larger than the experimental errors (a) and (b) or comparable with ones (b) and (c).

crease, was observed for all samples except for the one with $x=0.75$. For this particular composition, no significant variations of the peak intensities were found in the whole temperature range.

For the compositions with $x=0.125$ and 0.25, the characteristic changes in the temperature dependence of the Bragg peak intensities below 50 K (upturn and decrease in intensity of (101)/(020) and upturn and much faster increase in intensity of (121)/(002) and (200) peaks) indicate the ordering of the magnetic moments in the A-sublattice parallel to the magnetic moments in the B-sublattice. The refinement of magnetic moment direction gives reliable result for the samples with $x=0.125$ and 0.25. The best fit is obtained for the B-site magnetic moments M_B along b-axis. For other compositions the reliable determination of the magnetic moment direction is not possible because of the pseudo-cubic lattice symmetry. Figure 6 shows an example of the temperature dependencies of the magnetic moments at A- and B-sites for the composition with $x=0.25$ and 0.50.

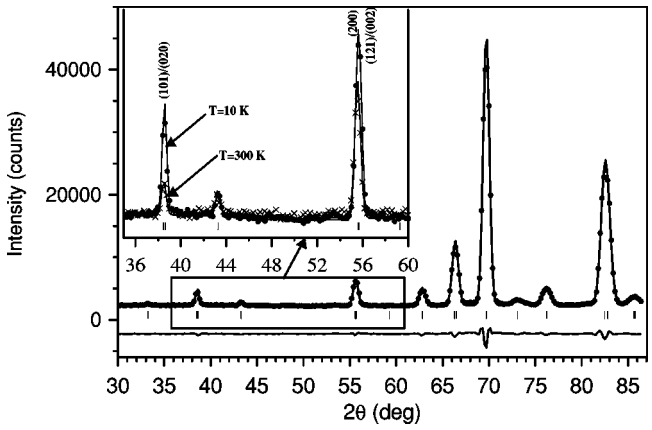

FIG. 5. Diffraction pattern of the $(Nd_{0.5}Sr_{0.5})(Mn_{0.5}Ru_{0.5})O_3$ sample, measured at the DMC at $T=10$ K and treated with the Rietveld method. Experimental points, calculated profile and difference function are shown. In the inset, the patterns (in 36–60 degree range) measured at 10 and 300 K are compared. The higher intensity at low temperature is due to the appearance of the FM ordering.

The ferromagnetic transition temperatures and the experimental low-temperature ($T=10$ K) magnetic moments for the A- and B-sites are listed in Table I. Ordering of the Nd (A-site) magnetic moments occurs only if the concentration of Nd is high enough ($1-x=0.875$ and 0.75). The experimental low-temperature ordered magnetic moment per one cation on a B-site can be properly described as $M_B(x)=|(1-x)\mu_{Mn}-x\mu_{Ru}|$ even for rough estimation with $\mu_{Mn}=4\mu_B$ ($t_{2g}^3e_g^1$ state) and $\mu_{Ru}=2\mu_B$ (low-spin t_{2g}^4 state). Such a description corresponds to the situation of anti-parallel ordering of Mn and Ru magnetic moments. Assumptions on the parallel ordering of Mn and Ru moments, or ordering of the solely Mn or Ru moments, cannot fit the experimental val-

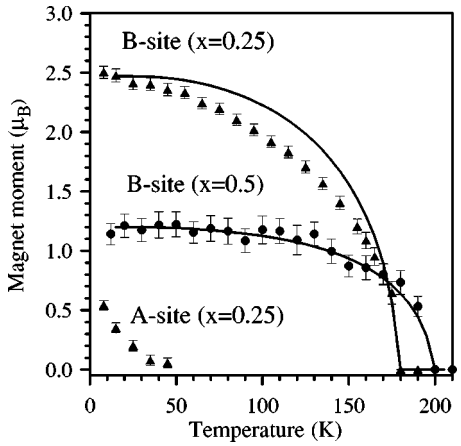

FIG. 6. Temperature dependence of the ordered magnetic moment in B-site (Mn/Ru) and A-site (Nd) for the sample with $x=0.25$ (▲), and B-site (Mn/Ru) for the sample with $x=0.5$ (•). The solid lines are results of the calculation according to the molecular field theory (see the discussion section).

TABLE I. Curie temperatures, T_{FM} (taken from neutron diffraction data, magnetic susceptibility data and calculations), experimental values of ordered magnetic moments for A- and B-sites (Nd/Sr and Mn/Ru, correspondingly), and calculated values for B-site, assuming antiferromagnetic interaction between Mn and Ru ions in $(Nd_{1-x}Sr_x)(Mn_{1-x}Ru_x)O_3$. Magnetic moments are given in Bohr magnetons. Calculations of M_{FM} are performed by $M_{FM}(x)=|(1-x)\mu_{Mn}-x\mu_{Ru}|$ for $\mu_{Mn}=3.74\ \mu_B$ and $\mu_{Ru}=1.34\mu_B$.

x	T_{FM}, K (B-site)			Experimental	Experimental	Calculated
	ND	$\chi(T)$	Calc.	M_{FM} for A-site	M_{FM} for B-site	M_{FM} for B-site
0.125	130(10)	120	135	1.00(4)	2.84(5)	3.10
0.25	180(5)	170	175	0.35(4)	2.49(4)	2.47
0.50	200(5)	200	210		1.14(5)	1.20
0.75		160	215		≈ 0	0.07
0.875	165(10)	160	190		0.41(1)	0.70
1[a]		160(10)	165		1.45	1.34

[a]Data from Refs. 21 and 23

ues. A reasonable correspondence between the experimental and calculated M_B values can be obtained if $\mu_{Mn}=4\ \mu_B$ and $\mu_{Ru}=1.45\ \mu_B$ are used. The last value is taken from spin-density functional theory calculation[21] for $SrRuO_3$. The fit of the experimental data to the linear function $M_B(x)=(1-x)\cdot\mu_{Mn}-x\mu_{Ru}$ gives $\mu_{Mn}=(3.74\pm0.15)\mu_B$ and $\mu_{Ru}=(1.34\pm0.25)\mu_B$. One can see (Fig. 7) that the experimental points are excellently fitted by straight line (except $x=0.125$) with the values of μ_{Mn} and μ_{Ru}, which are in good agreement with the expected magnetic moments of Mn and Ru. Results of the calculation are also listed in Table I.

In the proposed model, the absence of any measurable magnetic moment in the $x=0.75$ composition is simply an effect of nearly ideal compensation of Mn and Ru contributions to the magnetic structure factors. Indeed, $M_{Mn}=(1-x)\mu_{Mn}=0.935\mu_B$, $M_{Ru}=x\mu_{Ru}=1.005\mu_B$ for $x=0.75$ and $\mu_{Mn}=3.74\mu_B$, $\mu_{Ru}=1.34\mu_B$. For anti-parallel ordering of Mn and Ru magnetic moments, the magnetic structure factors are proportional to the difference $|M_{Mn}-M_{Ru}|=0.07\mu_B$ which is too small to be measured in the powder diffraction experiment.

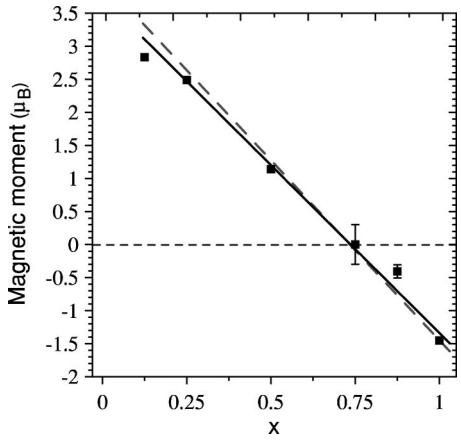

FIG. 7. Dependence of the ordered magnetic moment on B-site (Mn/Ru) of $(Nd_{1-x}Sr_x)(Mn_{1-x}Ru_x)O_3$ on the (Sr,Ru) content x. For $x=0.125$, 0.25, 0.50, 0.75, and 0.875, the values obtained in the present paper are shown. The value $\mu_{Ru}=1.45\mu_B$ for $x=1$ is taken from Ref. 21. The dashed line is calculation for theoretical values $\mu_{Mn}=4\mu_B$ and $\mu_{Ru}=1.45\mu_B$, the solid line is the least square approximation (in the $0.25\leqslant x\leqslant 1.0$ range) by linear function with $\mu_{Mn}=3.74\mu_B$ and $\mu_{Ru}=1.34\mu_B$.

To prove the presence of frozen magnetic moments and better identification of the temperature magnetic state of the $x=0.75$ sample we have exploited also the μSR technique. The μSR measurements with the same sample have been carried out using DOLLY spectrometer on the μE4 beam line at PSI. The powder sample was packed in an aluminum container, mounted in the helium flow cryostat.

No spontaneous muon spin precession in zero external magnetic field (ZF) was detected at low temperatures. The ZF muon spin polarization function $P(t)$ is rapidly relaxed at initial times (<10 ns), making practically impossible to study the fast relaxing part of $P(t)$. However, this behavior of the polarization function proves that the magnetic moments of Mn^{3+} and Ru^{4+} are static at low temperature, thus confirming the idea of the B-sublattice ferromagnetic moment compensation following from the ND data. Due to the large magnetic moment of Mn^{3+}, the local magnetic fields at the muon in the perovskite manganites are expected to be very large [e.g., the muon precession frequency $\sim$80 MHz is observed in $La_{0.67}Ca_{0.33}MnO_3$ (Ref. [24]) corresponds to the local field of $\sim$5 kG]. Due to the strong local disorder the dispersion of the local magnetic fields is large leading to the completely relaxed $P(t)$ at $t>10$ ns.

The sample volume occupied by the magnetically ordered state is better determined in the transverse external field (TF) experiment in the weak magnetic field of 100 Oe, which is much less than the internal magnetic field. The asymmetry (or amplitude) A_{TF} of the muon spin precession with the frequency corresponding to the external magnetic field is a direct measure of the paramagnetic volume fraction. Figure 8 shows the temperature dependence of A_{TF} together with magnetic susceptibility in $(Nd_{0.25}Sr_{0.75})(Mn_{0.25}Ru_{0.75})O_3$. The values of A_{TF} are given for the muon spin polarization component perpendicular to the initial muon spin polarization direction. For this component, any contribution from the magnetically ordered (short or long-range) regions of the sample volume is averaged to zero. Above 170 K the whole sample volume is in the paramagnetic state and the precession asymmetry is given by the total experimental asymme-

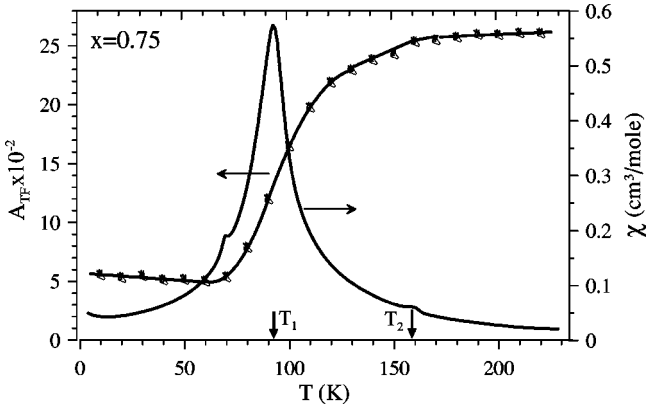

FIG. 8. Temperature dependence of the asymmetry (or amplitude) A_{TF} of the muon spin precession in the transverse external magnetic field of 100 Oe (left scale) and magnetic susceptibility (right scale) for $(Nd_{0.25}Sr_{0.75})(Mn_{0.25}Ru_{0.75})O_3$ ($x=0.75$ sample). The temperatures of two peculiarities are indicated according the magnetic susceptibility data.

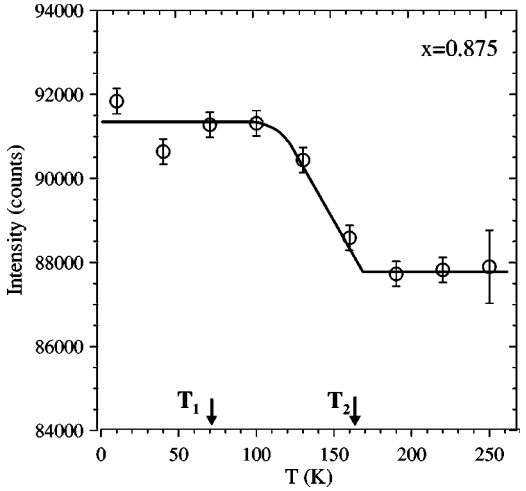

FIG. 9. Temperature dependence of the sum of the integrated intensities of the (101)/(020) and (200)/(121)/(002) Bragg peaks in the $x=0.875$ sample. The T_1 and T_2 transition temperatures are taken from the peculiarities in the magnetic susceptibility.

try $A_{TF}=0.26$. Below $T_2=160$ K which corresponds to a peculiarity in the magnetic susceptibility $\chi(T)$, the frozen atomic magnetic moments begin to appear in the part of the sample volume, causing the decrease in A_{TF}. Below $T \approx 115$ K, the $A_{TF}(T)$ curve changes its slope, becoming more rapidly decreasing function. The temperature $T_1 \approx 92$ K of the maximum of $\chi(T)$ roughly corresponds to the middle of the transition by $A_{TF}(T)$. The residual muon spin precession asymmetry at low temperature $A_{TF}=0.05$ ($\sim 20\%$) gives the fraction of the muon stops in the sample holder and in the part of sample volume which remained paramagnetic.

The slow relaxing part of the ZF polarization function has an exponential form $P_{ZF}=A_{ZF}\exp(-\lambda t)$ with noticeable $\lambda \simeq 0.2 \ \mu s^{-1}$ even at the low temperatures $T \leqslant 50$ K, implying that a slow dynamics of the local fields is present. The asymmetry A_{ZF} well corresponds to the expected 1/3 of the total experimental asymmetry.

For the sample with $x=0.75$ we cannot assign the ferromagnetic transition temperature to either T_1 or T_2. However, a comparison the susceptibilities of the samples with $x=0.75$ and $x=0.875$ shows that the both compositions have two peculiarities at the temperatures T_1 and T_2. The transition at T_2 in the sample with $x=0.875$ well corresponds to the ferromagnetic Curie temperature T_C determined from the temperature dependence of the integrated neutron intensities (Fig. 9). Since the net ferromagnetic moment in the sample with $x=0.875$ is small we present in Fig. 8 the sum of two most intense ferromagnetic Bragg peaks. By analogy we can assign the transition at T_2 to the ferromagnetic Curie temperature in the sample with $x=0.75$. The transition at $T=T_1$ is not revealed in the neutron diffraction data, and thus is probably related to a spin-glass-like or another short-range ordering effects.

IV. DISCUSSION

Good correspondence between the model calculations and the experimental data in the wide interval of Sr/Ru concentrations allows us to conclude that proposed interactions and obtained magnetic moments are intrinsic properties of Mn and Ru ions in the compound. The deviation of $x=0.125$ point is natural; for the small values of x the compound has to turn into the noncollinear (mainly A-type antiferromagnetic) state with close to zero ferromagnetic component of the ordered moment at B-site.[19] For the undoped $NdMnO_3$ compound, an antiferromagnetic A-phase is stabilized due to the orbital ordering and its energy is only slightly lower than the energy of FM order. Ru^{4+} is not Jahn-Teller active ion and serves as a defect for the orbitally ordered state. Therefore, even at small concentration of Ru^{4+}, the AFM order turns into FM.

As follows from the fitting procedure discussed above, the resulting interaction between the Mn and Ru ions should be antiferromagnetic. The nature of such an interaction can be understood by considering electron energy levels for both manganese and ruthenium ions. Their reference energies are $\varepsilon_{3d}^{Mn}=-15.27$ eV and $\varepsilon_{4d}^{Ru}=-14.59$ eV, correspondingly. These energies are very close to each other and allowing a significant overlapping between some of the orbitals. As Ru ion is in the low spin configuration, the crystal field splitting is essential and Ru e_g orbitals have rather high energy. As a result they are located high above the Mn e_g states and do not cross their Fermi energy and do not participate in the formation of the band. Thus the ferromagnetic superexchange between quarter-filled e_g band of Mn^{3+} and empty e_g band of Ru is suppressed. The resulting exchange between Ru and Mn ions is therefore the superexchange between half-filled $t_{2g}(3d)$ band of Mn and more than half-filled $t_{2g}(4d)$ band of Ru which should be antiferromagnetic according to Goodenough–Kanamori rules. Note, that if e_g states of Ru would lie close enough to the e_g states of Mn, the double exchange mechanism would work fine, Ru and Mn ions would be ferromagnetically coupled, and compound would show metallic behavior (see, for example, Ref. 10).

The antiferromagnetic superexchange interaction between Mn and Ru gives a state with a finite magnetic moment

which temperature dependence can be described in frame of the molecular field theory.[25] Let us divide the lattice of magnetic atoms (B-sites) into two "statistical sublattices" B1 and B2 such that Mn^{3+} and Ru^{4+} occupy the B1 and B2 sites correspondingly. Since Mn and Ru ions are located randomly in the whole volume of the compound, we are using the term "sublattices" only for convenience. We consider the case of a magnetically isotropic crystal with ferromagnetic interaction within both sublattices and antiferromagnetic interaction between them. The Hamiltonian of the system can be written as

$$H = -J_{11}\sum \mathbf{S}_{1i}\mathbf{S}_{1j} - J_{22}\sum \mathbf{S}_{2i}\mathbf{S}_{2j} + J_{12}\sum \mathbf{S}_{1i}\mathbf{S}_{2j}. \quad (1)$$

Here J_{11} and J_{22} are ferromagnetic exchange constants for Mn-Mn and Ru-Ru, respectively, and J_{12} is antiferromagnetic exchange constant Mn-Ru, $\mathbf{S}_1$ and $\mathbf{S}_2$ are the spin operators of Mn^{3+} and Ru^{4+} ions, the sums are taken over nearest neighbors of corresponding sublattices. The system of molecular field equations may be written in the form:

$$\begin{aligned} \alpha_1 &= z(1-x)J_{11}S_1\sigma_1 + zxJ_{12}S_2\sigma_2, \\ \alpha_2 &= zxJ_{22}S_2\sigma_2 + z(1-x)J_{12}S_1\sigma_1, \end{aligned} \quad (2)$$

where $z=6$ is the coordination number, and $\sigma_{1(2)}$ are relative magnetizations per site in sublattices B1(2):

$$\sigma_1 = 1 - B_{S1}(\alpha_1/T)/S_1, \quad \sigma_2 = 1 - B_{S2}(\alpha_2/T)/S_2, \quad (3)$$

B_S is the Brillouin function:

$$B_s(x) = \frac{\sum_{n=0}^{2s} ne^{-nx}}{\sum_{n=0}^{2s} e^{-nx}}. \quad (4)$$

This system of equations must be solved self-consistently to give σ_1 and σ_2 as functions of temperature T. The total magnetization can be written as

$$M = M_1 - M_2 = M_{10}\sigma_1 - M_{20}\sigma_2, \quad (5)$$

where $M_{10}=(1-x)S_1\mu_{Mn}$ and $M_{20}=xS_2\mu_{Ru}$, x is a concentration of Ru, μ_{Mn} and μ_{Ru} are magnetic moments of Mn and Ru ions. We performed the calculations with experimentally obtained values $\mu_{Mn}=3.74\ \mu_B$ and $\mu_{Ru}=1.34\ \mu_B$. From the experimental value of the Curie temperature $T_C=160$ K[22,23] in $SrRuO_3$ we calculate the Ru-Ru exchange constant $zJ_{22}=21$ meV using the above formulas of the molecular field approximation. The ferromagnetic superexchange between Mn ions was fixed to $zJ_{11}=2.1$ meV. This value is in the range reported in the literature for the planar ferromagnetic exchange in $LaMnO_3$.[26] The antiferromagnetic exchange J_{12} was considered as a free parameter. Good agreement with the experimental temperature dependencies of magnetization has been obtained with $zJ_{12}=23$ meV (Fig. 6). The calculated values of T_C are shown in Table I together with the experimentally measured ones.

Calculations reproduce satisfactorily well the temperature dependencies of magnetic moments, in particular for $x=0.25$ and $x=0.5$. However, there is a difference between calculated and experimentally measured values of $M(T)$. This quantitative disagreement can be understood as a consequence of the mean field approximation which neglects spin fluctuations and overestimates total magnetic moments $M_1(T)$ and $M_2(T)$ both for Mn- and Ru-sublattices. However since Mn ions have larger value of spin $S_1=2$ the molecular field theory is working better for Mn-sublattice than for Ru-sublattice with $S_2=1$. Moreover at low doping Ru ions can be considered as impurities for Mn-sublattice which worsens the application of the mean field theory. As a result, the magnetization $M_2(T)$ of Ru-sublattice is significantly overestimated. As Mn- and Ru-sublattices are antiferromagnetically coupled, the calculated total magnetic moment is under- or overestimated depending on the sign of total magnetic moment $M(T)$.

V. SUMMARY

Neutron diffraction, μSR, and electrical resistivity measurements have been performed to study the magnetic, structural, and electrical properties of $NdMnO_3$ upon simultaneous and consistent doping of A- and B- sites by Sr and Ru, respectively. The end members of the series $(Nd_{1-x}Sr_x)(Mn_{1-x}Ru_x)O_3$ are A-type antiferromagnetic insulator ($x=0$) and ferromagnetic metal ($x=1$). The Sr and Ru doping assures an increase of the tolerance factor at higher x, which must favor an appearance of the metallic state. Nevertheless, the metallic state in our samples is not present, they are all insulators, and we do not observe any peculiarities on the resistivity curves at magnetic transition temperatures. This implies, that the DE mechanism, which is practically excluded in $(Nd_{1-x}Sr_x)(Mn_{1-x}Ru_x)O_3$, is very important for correlation between FM order and metallic state as it is well known for the doped manganites.

Good correspondence between the experimental data and model calculations for the low-temperature Mn and Ru magnetic moments as function of (Sr/Ru) concentration in a wide range of x, indicates that hypothesis about FM correlation magnetic moments within both Mn-Mn and Ru-Ru pairs and AFM correlation of the moments in Mn-Ru pairs is correct. The electronic states are $t_{2g}^3e_g^1$ for Mn^{3+} and low-spin $t_{2g}^4e_g^0$ for Ru^{4+}, respectively, with quite different values of the moments: $\mu_{Mn}=3.74(15)\mu_B$ and $\mu_{Ru}=1.34(25)\mu_B$. Due to random distribution of Mn and Ru over B-sites (as it follows from diffraction patterns) the obtained magnetic state can be called "statistical ferrimagnet." The concentration dependencies of the ferromagnetic transition temperatures and the saturated magnetic moments calculated in the mean field approximation are in rather good agreement with the proposed magnetic state.

The discovered unusual interaction between Mn and Ru magnetic moments can provide also a new insight to the anomalies of the ferromagnetic state which were observed in Ru doped perovskite manganites earlier (see Ref. 6 for review).

ACKNOWLEDGMENTS

The authors are grateful to P. Fischer and N. M. Plakida for helpful discussions. The work was done with the help of the Russian program RFBR (projects 00-02-16736 and 02-03-33258), the INTAS foundation (project 01-2008) and the Swiss foundation SNSF (project 7SUPJ062190.00/1). This work was partially performed at the spallation neutron source SINQ, Paul Scherrer Institut, Villigen, Switzerland.

*Electronic mail: bushme@nf.jinr.ru

†On leave from Frank Laboratory of Neutron Physics, JINR, 141980, Dubna, Moscow region, Russia.

[1] J. M. D. Coey, M. Viret, S. von Molnar, Adv. Phys. **48**, 167 (1999).

[2] M. B. Salamon and M. Jaime, Rev. Mod. Phys. **73**, 583 (2001).

[3] C. Zener, Phys. Rev. **82**, 403 (1951).

[4] Guo-meng Zhao, Phys. Rev. B **62**, 11 639 (1996).

[5] C. Martin, A. Maignan, M. Hervieu, C. Autret, B. Raveau, and D. I. Khomskii, Phys. Rev. B **63**, 174402 (2001).

[6] B. Raveau, A. Maignan, C. Martin, and M. Hervieu, J. Supercond. **14**, 217 (2001).

[7] Ranjan K. Sahu, Z. Hu, Manju L. Rao, S. Sundar Manoharan, T. Schmidt, B. Richter, M. Knupfer, M. Golden, J. Fink, and C. M. Schneider, Phys. Rev. B **66**, 144415 (2002).

[8] F. Weigand, S. Gold, A. Schmid, J. Geissler, E. Goering, K. Dörr, G. Krabbes, and K. Ruck, Appl. Phys. Lett. **81**, 2035 (2002).

[9] S. C. Gausepohl, M. Lee, K. Char, R. A. Rao, and C. B. Eom, Phys. Rev. B **52**, 3459 (1995).

[10] B. Raveau, A. Maignan, C. Martin, R. Mahendiran, and M. Hervieu, J. Solid State Chem. **151**, 330 (2000).

[11] Kannan M. Krishnan and H. L. Ju, Phys. Rev. B **60**, 14 793 (1999).

[12] L. S. Lakshmi, V. Sridharan, D. V. Natarajan, Sharat Chandram, V. Sankara Sastry, T. S. Radhakrishnani, Ponn Pandian, and A. Narayanasamy, cond-mat/0204441.

[13] A. A. Bosak, O. Yu. Gorbenko, A. R. Kaul, I. E. Graboy, C. Dubourdieu, J. P. Senateur, and H. W. Zandbergen, J. Magn. Magn. Mater. **211**, 61 (2000).

[14] J. A.M. Van Roosmalen, E. H.P. Cordfunke, and R. B. Helmholdt, J. Solid State Chem. **110**, 100 (1994).

[15] P. Fischer, G. Frey, M. Koch, M. Koennecke, V. Pomjakushin, J. Schefer, R. Thut, N. Schlumpf, R. Buerge, U. Greuter, S. Bondt, and E. Berruyer, Physica B **276–278**, 146 (2000).

[16] V. B. Zlokazov and V. V. Chernyshev, J. Appl. Crystallogr. **25**, 447 (1992).

[17] T. Roisnel and J. Rodríguez-Carvajal, Mater. Sci. Forum **378**, 118–123 (2001).

[18] V. A. Amelichev, O. Yu. Gorbenko, A. R. Kaul, E. A. Gan'shina, A. M. Balagurov, S. N. Bushmeleva, V. Yu. Pomjakushin, D. V. Sheptyakov, N. A. Babushkina, L. M. Belova, and K. V. Rao, J. Solid State Chem. (to be published).

[19] S. Y. Wu, C. M. Kuo, H. Y. Wang, W.-H. Li, K. C. Lee, J. W. Lynn, and R. S. Liu, J. Appl. Phys. **87**, 5822 (2000).

[20] C. W. Jones, P. D. Battle, P. Lightfoot, and W. T.A. Harrison, Acta Crystallogr., Sect. C: Cryst. Struct. Commun. **45**, 365 (1989).

[21] P. B. Allen, H. Berger, O. Chauvet, L. Forro, T. Jarlborg, A. Junod, B. Revaz, and G. Santi, Phys. Rev. B **53**, 4393 (1996).

[22] A. Kanbayasi, J. Phys. Soc. Jpn. **41**, 1876 (1976).

[23] J. M. Longo, P. M. Raccah, and J. B. Goodenough, J. Appl. Phys. **39**, 1327 (1968).

[24] R. H. Heffner, L. P. Le, M. F. Hundley, J. J. Neumeier, G. M. Luke, K. Kojima, B. Nachumi, Y. J. Uemura, D. E. MacLaughlin, and S.-W. Cheong, Phys. Rev. Lett. **77**, 1869 (1996).

[25] S. V. Tyablikov, *Methods in the Quantum Theory of Magnets* (Plenum, New York, 1967).

[26] L. F. Feiner and A. M. Oles, Phys. Rev. B **59**, 3295 (1999).